Trans Fatty Acid Derived Phospholipids Show Increased Membrane Cholesterol and Reduced Receptor Activation as Compared to Their Cis Analogs

3 AUTHORS, INCLUDING:

Drake C Mitchell
Portland State University
59 PUBLICATIONS **2,610** CITATIONS

SEE PROFILE

Burton Litman
National Institutes of Health
83 PUBLICATIONS **6,030** CITATIONS

SEE PROFILE

Trans Fatty Acid Derived Phospholipids Show Increased Membrane Cholesterol and Reduced Receptor Activation as Compared to Their Cis Analogs

Shui-Lin Niu[*], **Drake C. Mitchell**, and **Burton J. Litman**[*]

Section of Fluorescence Studies, Laboratory of Membrane Biochemistry and Biophysics, National Institute on Alcohol Abuse and Alcoholism, National Institutes of Health, Rockville, Maryland 20852

Abstract

The consumption of trans fatty acid (TFA) is linked to the elevation of LDL cholesterol and is considered to be a major health risk factor for coronary heart disease. Despite several decades of extensive research on this subject, the underlying mechanism of how TFA modulates serum cholesterol levels remains elusive. In this study, we examined the molecular interaction of TFA-derived phospholipid with cholesterol and the membrane receptor rhodopsin in model membranes. Rhodopsin is a prototypical member of the G-protein coupled receptor family. It has a well-characterized structure and function and serves as a model membrane receptor in this study. Phospholipid–cholesterol affinity was quantified by measuring cholesterol partition coefficients. Phospholipid–receptor interactions were probed by measuring the level of rhodopsin activation. Our study shows that phospholipid derived from TFA had a higher membrane cholesterol affinity than their cis analogues. TFA phospholipid membranes also exhibited a higher acyl chain packing order, which was indicated by the lower acyl chain packing free volume as determined by DPH fluorescence and the higher transition temperature for rhodopsin thermal denaturation. The level of rhodopsin activation was diminished in TFA phospholipids. Since membrane cholesterol level and membrane receptors are involved in the regulation of cholesterol homeostasis, the combination of higher cholesterol content and reduced receptor activation associated with the presence of TFA–phospholipid could be factors contributing to the elevation of LDL cholesterol.

Trans fatty acid (TFA),[1] the stereoisomer of the naturally occurring cis fatty acid (CFA), is considered to be a major health risk factor for coronary heart disease. TFA and CFA are stereoisomers that only differ in the geometry of the CdC double bond. TFA adopts a more linear configuration similar to that of saturated fatty acid, while CFA adopts a bent configuration (illustrated in Figure 1). The linear configuration of TFA allows stronger intermolecular chain–chain interaction, resulting in a higher transition temperature for TFA chain melting (1). TFA is mainly produced by partial hydrogenation of unsaturated oils and is widely found in a variety of foods, including margarines, vegetable shortening, frying oils, etc. (2). The average American consumes more than 5 g of TFA daily, which is equivalent to ~7% of total fat consumption (3). It is widely documentedÌthat TFA is incorporated in serum lipids, lipoproteins, and adipose tissues in the form of triglyceride, phospholipids, and cholesterol esters (4-10), although the efficiency of incorporation varied among different tissues or lipid forms. The dietary intake of TFA is associated with the elevation of LDL cholesterol (11-15) and increased risk for coronary heart disease (16-18). However, the cause for LDL cholesterol elevation by TFA, or in a more general scope, the cause for LDL cholesterol regulation by fatty acid, is not well-understood. In the past several decades, extensive studies have been conducted

[*]Corresponding authors. (S.-L.N.) Tel: (301) 435-6728. Fax: (301) 594-0035. E-mail: sniu@niaaa.nih.gov. (B.J.L.) Tel: (301) 594-3608. Fax: (301) 594-0035. E-mail: litman@helix.nih.gov.

on how different fatty acid intake affects the pathways of cholesterol adsorption (19), cholesterol metabolism (20), and cholesterol biosynthesis (21). However, no conclusive mechanism has been determined yet.

Previous studies show that membrane cholesterol concentration (22,23) or activity (24) is modulated by membrane phospholipid composition due to the differential interactions of phospholipids with cholesterol (25-29). The composition of membrane phospholipids also influences the physical properties and function of membrane proteins (30,31). However, it is not known whether the presence of TFA-derived phospholipids in membranes, resulting from the dietary intake of TFA, affects the membrane affinity for cholesterol and membrane protein function. In this study, the molecular interactions of TFA- and CFA-containing phospholipids with cholesterol and their effect on membrane receptor activation were investigated in model membranes. The interactions of TFA- and CFA-phospholipids with cholesterol were quantified using equilibrium cholesterol partition coefficients, while the effect of these phospholipids on membrane receptor stability was characterized using differential scanning calorimetry in reconstituted rhodopsin-containing vesicles, consisting of TFA- or CFA-phospholipids. Membrane receptor function was measured by the level of rhodopsin activation in these reconstituted vesicles. Since rhodopsin is a prototypical member of the G protein coupled receptor (GPCR) family with well-characterized structure and function (32), conclusions

---

[1]Abbreviations:

CD
methyl-β-cyclodextrin;

CFA
cis fatty acid;

di-18:1n9(c)PC
1,2-dioleoyl-*sn*-glycero-3-phosphocholine;

di-18:1n9-(t)PC
1,2-dielaidoyl-*sn*-glycero-3-phosphocholine;

DHA
docosahexaenoic acid;

DSC
differential scanning calorimetry;

K_{CD}^{LUV}
cholesterol partition coefficient between CD and lipid bilayers;

K_{cis}^{trans}
cholesterol partition coefficient between lipid bilayers consisting of *trans*- and *cis*-phospholipids;

K_{eq}
equilibrium constant for metarhodopsin I (MI) and metarhodopsin II (MII) equilibrium;

LUV
large unilamellar vesicles;

SCAP
SREBP cleavage activating protein;

SREBP
sterol regulatory element binding proteins;

TFA
trans fatty acid;

T_m
phase transition temperature.

drawn from our study of rhodopsin may be generalized to other membrane receptors in this family, as well as other integral membrane receptors.

Our study found that TFA–phospholipids had a higher cholesterol affinity, resulting in a higher level of cholesterol incorporated in these membranes relative to that in the CFA–phospholipid membrane. TFA–phospholipids also ordered membrane acyl chain packing, which is reflected by the reduced membrane acyl chain packing free volume and the higher transition temperature for the thermal unfolding of rhodopsin. The increase in acyl chain packing order is associated with a reduced level of rhodopsin activation, consistent with a previously established link between membrane free volume and rhodopsin activation (30).

EXPERIMENTAL PROCEDURES

Sample Preparation.

Phospholipids were purchased from Avanti Polar Lipids (Alabaster, AL); cholesterol and methyl-β-cyclodextrin (CD) were from Sigma (St. Louis, MO); and the cholesterol–CD complex was freshly prepared as described earlier (23). The cholesterol CII assay kit was from Wako (Wako Chemicals USA, Inc., Richmond, VA). Unless otherwise stated, all samples were in pH 7.0 PBS buffer, which contained 10 mM PIPES, 30 mM NaCl, 60 mM KCl, and 50 μM DTPA. Phospholipids were lyophilized under vacuum and hydrated in PBS buffer, which spontaneously formed multilamellar vesicles. The multilamellar vesicles were forced through double layers of 0.1 μm polycarbonate filters 11 times, which yielded unilamellar (LUV) vesicles with an average diameter of 100 nm (23). The photoreceptor rhodopsin was purified on a Concanavalin-A affinity column (33) from rod outer segments (ROS), which were isolated from frozen bovine retinas (James and Wanda Lawson, Lincoln, NE) (34). Reconstituted rhodopsin-containing lipid vesicles were prepared using the rapid dilution technique (35). A molar ratio of 100 lipids per protein was maintained for all protein-containing vesicles. Each vesicle preparation was assayed for phospholipid (36) and rhodopsin (37). The variation of lipid-to-protein ratio among different preparations was normally less than 5%. Since rhodopsin is light sensitive, all sample preparations and measurements were carried out in the dark with the aid of night vision goggles.

Phospholipid-Cholesterol Affinity Determination.

Phospholipid-cholesterol affinities were quantified by the equilibrium cholesterol partition coefficients, using a recently developed method (23). Briefly, LUV consisting of the TFA–phospholipid or the CFA–phospholipid were incubated with the cholesterol–CD complex, which serve as the cholesterol donor. Spontaneous cholesterol transfer from CD to lipid vesicle occurred until the establishment of an equilibrium, which takes place in less than an hour. The cholesterol donor CD was then separated from the cholesterol acceptor LUV by membrane filtration based on their size differences. The equilibrium concentrations of cholesterol in CD and LUV were determined using a Cholesterol CII kit, and the equilibrium cholesterol partition coefficient K_{CD}^{LUV} was determined accordingly. The relative cholesterol partition between TFA–phospholipid vesicles and *cis*-phospholipid was calculated as $K_{cis}^{trans} = K_{CD}^{trans}/K_{CD}^{cis}$. All measurements were carried out at 37 °C in PBS buffer, pH 7.0 and repeated for a minimum of three trials.

Differential Scanning Calorimetry (DSC) Measurements.

DSC measurements were conducted in a Nano-Scan II calorimeter (Calorimetry Sciences Co., Provo, UT) equipped with capillary sample compartments. Rhodopsin containing vesicles at a concentration of 0.5 mg/mL rhodopsin in pH 7.0 PBS buffer were degassed and loaded into sample cell in complete dark. The cell was sealed under a stream of argon and pressurized to 2.8 atm. A total of four scans (two heating scans and two cooling scans) at a scan rate of 0.25°

C/min from 0 to 80°C was collected for each sample. Each sample was repeated twice for DSC measurement. Reference scans using PBS buffer were conducted under identical conditions and were subtracted from sample scans. The data were exported and analyzed using Origin 7.0 (OriginLab Corp., Northampton, MA).

Time-Resolved Fluorescence Measurements.

The acyl chain packing property of membranes consisting of TFA–phospholipid or CFA–phospholipid was determined using time-resolved anisotropy decay of the fluorescent probe DPH (38,39). Briefly, DPH was added into membranes at the lipid-to-probe ratio of 500:1 in PBS buffer. DPH lifetime and differential polarization data were collected at 37°C in an ISS K2 multifrequency cross-correlation phase fluorometer (ISS, Urbana, IL). The time-resolved anisotropy decay was analyzed using the sum-of-exponential and the BRD model. The parameter, $f_{v'}$, which is defined as $f_{v'}$ $(2 f(\Theta)_{max})^{-1}$, was used to quantify the extent to which the equilibrium orientational freedom of DPH is restricted by the phospholipid acyl chains (38,39).

Rhodopsin Activation Measurements.

Rhodopsin activation was determined from the equilibrium spectra of metarhodopsin I (MI) and metarhodopsin II (MII), the inactive and active photointermediates of light activated rhodopsin, respectively. The MI-MII equilibrium spectra were derived from a set of UV/vis absorbance spectra of rhodopsin as previously described (40). The equilibrium constant (K_{eq}) was expressed as $K_{eq}[MII][MI]$. K_{eq} was determined at several temperatures in pH 7.0 PBS buffers that were corrected for the temperature variation of the pK_a of PIPES.

Miscellaneous Assays.

Phospholipid concentration was determined by total phosphate using the method of Barlett (36). The rhodopsin concentration was determined by absorbance at 500 nm using an extinction coefficient of 40 000 M cm^{-1} (37).

RESULTS

Determination of Phospholipid-Cholesterol Affinity.

Three pairs of phosphatidylcholine (PC), di-14:1n5PC, di-16: 1n7PC, and di-18:1n9PC, where each pair consists of stereoisomers with a double bond in either the cis or the trans geometry, were used to compare cholesterol affinities. Equilibrium cholesterol partition coefficients were determined in a two-component system containing LUV and a cholesterol/CD complex as previous described (23). When LUV consisting of TFA–phospholipid or CFA-phospholipid were incubated with a cholesterol donor, cholesterol–CD complexes, cholesterol spontaneously transferred into LUV until an equilibrium distribution was reached. The equilibrium cholesterol partition coefficient between LUV and CD, K_{CD}^{LUV}, which is the quantitative measurement of cholesterol affinity, is shown in Figure 2A. K_{CD}^{LUV} was 3.54 ± 0.07 for LUV consisting of CFA–phospholipid, di-18: 1n9(c)PC, indicating that cholesterol partitions 3.54-fold more into the LUV than into CD, when both LUV and CD are present in equal molar quantities. When the same measurement was carried out in LUV consisting of TFA–phospholipid, di-18:1n9(t)PC, K_{CD}^{LUV} was increased to 6.29 ± 0.03. The relative cholesterol partition coefficient, K_{cis}^{trans}, between di-18:1n9(t)PC LUV and di-18:1n9(c)PC LUV was 1.78, demonstrating that the TFA–phospholipid has a higher cholesterol affinity than the CFA–phospholipid. Similar results were obtained in di-14:1n5PC and di-16:1n7PC vesicles (Figure 2B). The K_{cis}^{trans} values were 1.43 and 1.69 for di-14:1n5PC and di-16:1n7PC, respectively. The corresponding extra partition free energies, $\Delta(\Delta G)$, for partitioning into the TFA phospholipid relative to the CFA phospholipid at physiological temperature (37°C) are

-220, -323, and -355 cal/mol for di-14:1n5PC, di-16:1n7PC, and di-18:1n9PC, respectively. This demonstrates the stronger interactions of cholesterol with TFA–phospholipids relative to CFA–phospholipids.

Time-Resolved DPH Fluorescence Measurements.

The fluorescence lifetime and anisotropy decay of DPH were summarized in Table 1. The average lifetime of DPH, $\langle\tau\rangle$, in the CFA–phospholipid (di18:1n9(c)PC), was 7.37±0.02 ns, similar to that previously reported (39). A longer $\langle\tau\rangle$, 8.28±0.23 ns, was observed in the TFA–phospholipid, di18:1n9(t)PC. This value is similar to that observed in 16: 0, 18:1n9(c)PC, which has a saturated chain at the *sn*-1 position, or in di18:1n9(c)PC with 30% (mol) cholesterol (29,39). These bilayers have a higher order of acyl chain packing than di18:1n9(c)PC, which results in a lower water penetration into the bilayers, resulting in a reduced quenching of DPH fluorescence.

The average rotational correlation time $\langle\phi\rangle$ of DPH, which was obtained from time-resolved anisotropy measurements and analyzed in terms of biexponential decay, differed by Ì~30% between di18:1n9(c)PC and di18:1n9(t)PC. $\langle\phi\rangle$ was longer in the TFA–phospholipid, indicating that the rotational diffusion of the DPH probe was slower. A similar result was obtained from the analysis of DPH anisotropy data using the BRD model. The rotational diffusion coefficient, $D_\perp$, was slightly higher in di18:1n9(c)PC, consistent with the lower value of $\langle\phi\rangle$. The membrane acyl chain packing free volume, f_v, was Ì~30% lower in di18:1n9(t)PC than that in di18:1n9(c)PC, indicating a higher order of acyl chain packing in the TFA–phospholipid.

Characterization of Phospholipid-Receptor Interaction.

Phospholipid-receptor interaction was characterized in reconstituted membranes containing rhodopsin and TFA- or CFA–phospholipid using differential scanning calorimetry. DSC scans were collected from 0 to 80°C, which covers the gel-to-fluid phase transition of di-18:1(t)PC and the thermal transition of rhodopsin denaturation. The phase transition temperature of di-18:1(c)PC is -11°C (41,42), which is beyond the scan range of our Nano-scan II calorimeter. Thus, the phase transition of di-18:1(c)PC was not resolved in this study. Figure 3A shows the region of rhodopsin denaturation in bilayers consisting of either di-8:1n9(t)PC or di-18:1n9(c) PC. The transition temperature (T_m) of rhodopsin denaturation in the di-18:1n9(c)PC bilayers was 68.0°C (Table 2), while the T_m was increased to 69.7°C in di-18:1n9(t)PC bilayers, 1.7° C higher than in di-18: 1n9(c)PC. The thermal denaturation of rhodopsin was also accompanied by a higher enthalpy value in the TFA–phospholipid, which is 198.5±1.2 kcal/mol in di-18:1n9-(t)PC versus 160.6±1.1 kcal/mol in di-18:1n9(c)PC (Table 2), further demonstrating the stabilization of rhodopsin toward thermal denaturation by the TFA–phospholipid.

The gel-to-liquid crystalline phase transition of pure di-18:1n9(t)PC bilayers was highly cooperative, evidenced by a single sharp transition band at 11.5°C (Figure 3B). In the presence of rhodopsin in bilayers, the gel-to-liquid crystalline phase transition of di-18:1n9(t)PC broadened significantly with two resolved transition peaks centered at 8.8 and 10.7°C, respectively (Figure 3B). NMR and ESR studies have reported the existence of two populations of phospholipids in native disk membranes and reconstituted rhodopsin-containing membranes (43-46). The phospholipids in direct contact with rhodopsin are motionally restricted, and as such, are distinct from the bulk phospholipids. The presence of two distinct lipid phase transitions in rhodopsin-containing membranes by DSC is consistent with the NMR and ESR results. Another interesting observation was that once rhodopsin was thermally denatured, it had less perturbation on the phase transition of di-18:1n9(t)PC. The rescan of the thermally denatured rhodopsin-containing vesicles exhibited a single symmetric transition band at 11.2° C (Figure 3B). This transition band was highly reproducible when the sample was subjected

for additional scans. Both T_m and ΔH values associated with the gel-to-liquid crystalline phase transition of di-18:1n9(t)PC in the presence of denatured rhodopsin were close to those of pure di-18:1n9(t)PC bilayers (Table 2), indicating weakened interactions between denatured rhodopsin and phospholipids as compared to that between native rhodopsin and phospholipids.

Characterization of Rhodopsin Activation.

The deconvolved equilibrium spectra of MI and MII acquired in reconstituted rhodopsin-containing bilayers consisting of either di-18:1n9(c)PC or di-18:1n9(t)PC are shown in Figure 4. MI and MII species have maximal absorption at 480 and 385 nm, respectively. It is obvious from the spectrum that di-18:1n9(c)PC bilayers supported more MII formation. The equilibrium constant for the MI-MII equilibrium, K_{eq}, which is a measure of the ratio of MII to MI, was reduced by 21% in di-18:1n9(t)PC relative to that in di-18:1n9(c)PC at 37°C (Figure 5). This difference was most pronounced at 5°C, where di-18:1n9(c)PC is in fluid phase and di-18:1n9-(t)PC is in gel phase. The K_{eq} value was 3-fold lower in di-18:1n9(t)PC relative to di-18:1n9(c)PC. At all temperatures measured in this study, K_{eq} values were consistently lower in di-18:1n9(t)PC bilayers (Figure 6).

The van't Hoff plot of ln K_{eq} versus $1/T$ in di-18:1n9(c)-PC bilayers followed a straight line (Figure 6), which yielded ΔH_{vh} and ΔS to be 10.44±0.42 kcal/mol and 33.44±1.45 kcal/mol K, respectively (Table 3). In di-18:1n9(t)PC bilayers, a linear correlation was only observed between 15 and 37°C, where di-18:1n9(t)PC is in the fluid phase. The corresponding ΔH_{vh} and ΔS values were higher than those in di-18:1n9(c)PC bilayers. The ln K_{eq} value obtained at 5°C ($1/T$) 3.6×10^{-3}, K^{-1}), where di-18:1n9(t)PC is in the gel phase, fell below the projected value from the van't Hoff plot, demonstrating an additional role of lipid phase transition in modulating rhodopsin activation.

DISCUSSIONS

TFA and CFA are stereoisomers of unsaturated fatty acids with one or more CdC double bonds in trans or cis geometry. The subtle difference in double bond geometry results in significant changes in phospholipid-cholesterol and phospholipid-membrane receptor interactions as shown in this study.

Our results show that TFA–phospholipids have a 40-80% higher cholesterol affinity than their cis analogues as determined from their cholesterol partition coefficients (Figure 2B). This indicates that the cholesterol level would be 40-80% higher in TFA–phospholipid membranes relative to CFA–phospholipid membranes. This result provides for the first time the quantitative difference in the acyl chain-cholesterol interaction based on the sole difference in double bond geometry. Previous studies, using phospholipids derived from either CFAs or saturated FAs, demonstrated that phospholipid-cholesterol interactions are greatly influenced by the phospholipid acyl chain composition (23, 27). Phospholipids with saturated acyl chains allow better van der Waals contact between phospholipid acyl chains and cholesterol, resulting in higher cholesterol affinity. In contrast, the presence of cis double bond(s) in acyl chains reduces the acyl chain-cholesterol interaction due to the unfavorable configuration of acyl chains induced by cis double bond(s). *Trans*-acyl chains adopt extended configurations similar to saturated acyl chains, allowing better interaction with the cholesterol molecule than their cis analogues (Figure 1). It is also interesting that the difference in cholesterol affinity between TFA- and CFA-phospholipids increases with increasing acyl chain length.

Our fluorescence measurements demonstrated that the acyl chain packing order is higher in di-18:1n9(t)PC membranes than in di-18:1n9(c)PC membranes (Table 1), which is reflected by the reduced DPH diffusional coefficient and lower acyl chain packing free volume. The DPH fluorescence lifetime is higher in di-18:1n9(t)PC membranes, indicating less water

penetration into the membranes, resulting in reduced quenching of DPH fluorescence. This agrees with the lower membrane permeability in the TFA–phospholipid (41). The higher acyl chain packing order in the TFA–phospholipid membranes is due to the favored van der Waals interactions among *trans*-acyl chains, which also explains the 30°C difference in phase transition temperature between di-18:1n9(t)PC and di-18:1n9(c)PC membranes (42,47).

Since rhodopsin and other membrane receptors are surrounded by a lipid matrix, the change of membrane physical property is expected to be influential to the structure and function of membrane receptors. We observed that the thermal denaturation temperature of rhodopsin was greater by 1.7°C in di-18:1n9(t)PC than in di-18:1n9(c)PC (Table 2). The size of the T_m shift by changing the geometry of the CdC double bond was comparable to the T_m shift induced by the addition of 30% (mol) cholesterol in rhodopsin-containing membranes (48). The level of rhodopsin activation was reduced by 21% in di-18:1n9(t)PC membranes relative to di-18:1n9(c)PC membranes at 37°C where both lipids are in the fluid phase. The reduction of K_{eq} in the di-18: 1n9(t)PC membranes correlated with the reduced f_v value observed for this phospholipid. This is consistent with the link between K_{eq} and f_v observed in previous studies (30). Since the activation of rhodopsin from the MI state to the MII state involves a large conformational change (49,50), membranes with lower f_v or higher acyl chain packing orders would impose a higher energy barrier for such conformational change; thus, a lower level of rhodopsin activation is expected. The reduction of rhodopsin activation was more pronounced at 5°C, where di-18:1n9(t)PC is in the gel state and di-18:1n9(c)PC is in the fluid state. The acyl chains are much more ordered in gel state than in the liquid crystalline state, resulting in a 3-fold difference in K_{eq} between di-18: 1n9(t)PC and di-18:1n9(c)PC. Since rhodopsin activation is the initial event in the G protein coupled visual signaling cascade, the reduction of rhodopsin activation by the TFA–phospholipids would result in a down regulation of the signaling pathway. Because a conformational change is generally required for receptor activation, the influence of the TFA–phospholipid on rhodopsin activation may be generalized to other GPCR pathways and is likely a factor in the function of other membrane receptors.

It is well-established that the dietary intake of TFA leads to the incorporation of TFA in a variety of tissues and various lipid forms including phospholipids. The results of this study demonstrate that the incorporation of TFA in phospholipids leads to an increase in membrane cholesterol levels and a reduction in membrane receptor activation. These effects could be contributing factors in modulating cholesterol homeostasis, and as such, may be part of the explanation of the elevation of LDL cholesterol by a TFA-rich diet. First, cholesterol homeostasis is maintained through LDL-receptor mediated endocytosis, a rate-limiting step for the removal of LDL cholesterol from serum (51). The activity of the LDL receptor could be modulated by the TFA–phospholipid in a fashion similar to rhodopsin as discussed previously since both receptors are integral membrane proteins surrounded by phospholipids. The reduction of LDL receptor activity would reduce the rate of LDL clearance from serum and result in higher LDL cholesterol in serum. Second, recent studies show that the cellular cholesterol level is regulated by an internal cholesterol sensor, SCAP (52). SCAP is a transmembrane protein located in the ER membrane containing a sterol-sensing domain (SSD), a common motif consisting of five transmembrane helices that is also found in three other cholesterol sensing proteins. SCAP detects the cellular cholesterol level and responds to the fluctuation of cellular cholesterol by switching the signaling pathway of cholesterol biosynthesis either on or off, thus maintaining a constant level of cellular cholesterol (52-54). Although the cholesterol binding site in SCAP has not been characterized yet, it is likely that the intrinsic cholesterol affinity of SCAP determines the operation of the sensor. The effective concentration of cholesterol or cholesterol activity in membranes is normally lower than the total membrane cholesterol concentration since cholesterol interacts and binds with phospholipids in membranes (24). TFA–phospholipids exhibit higher cholesterol affinity than CFA–phospholipids, so the cholesterol activity in the TFA–phospholipid membranes will be

lower than in the CFA–phospholipid membranes. To reach the same physiological level of cholesterol activity that triggers the response of SCAP, a higher concentration of total membrane cholesterol would be required in the TFA–phospholipid membranes. Thus, the system indirectly increases the absolute cholesterol threshold for SCAP, allowing more cholesterol to be synthesized before the pathway for cholesterol biosynthesis is turned off. As a consequence, a higher level of cholesterol is maintained in the TFA–phospholipid membranes than that in the CFA–phospholipid membranes.

In summary, this study demonstrates that TFA–phospholipids exhibit higher cholesterol affinity than their stereoisomer CFA–phospholipids. Membranes containing TFA–phospholipids have a higher order of acyl chain packing and diminish membrane receptor activation. The fundamental differences between TFA- and CFA–phospholipids observed here in model membranes is worth investigating in in vivo systems. This would aid in clarifying the role played by dietary fat in the regulation of cholesterol homeostasis.

REFERENCES

1. Small, DM.; Steiner, J. The physical chemistry of lipids. From Alkanes to phospholipids. Handbook of lipid research. Plenum Press; New York: 1986. p. 587-592.

2. Expert Panel. Trans fatty acids and coronary heart disease risk. Report of the expert panel on trans fatty acids and coronary heart disease. Am. J. Clin. Nutr 1995;62:655S–708S. [PubMed: 7661131]

3. Allison DB, Egan SK, Barraj LM, Caughman C, Infante M, Heimbach JT. Estimated intakes of trans fatty and other fatty acids in the U.S. population. J. Am. Diet. Assoc 1999;99:166–174. [PubMed: 9972183]

4. Schrock CG, Connor WE. Incorporation of the dietary trans fatty acid (C18:1) into the serum lipids, the serum lipoproteins, and adipose tissue. Am. J. Clin. Nutr 1975;28:1020–1027. [PubMed: 169685]

5. Privett OS, Phillips F, Shimasaki H, Nozawa T, Nickell EC. Studies of effects of trans fatty acids in the diet on lipid metabolism in essential fatty acid deficient rats. Am. J. Clin. Nutr 1977;30:1009–1017. [PubMed: 879068]

6. Cook HW. Incorporation, metabolism, and positional distribution of trans-unsaturated fatty acids in developing and mature brain. Comparison of elaidate and oleate administered intracerebrally. Biochim. Biophys. Acta 1978;531:245–256. [PubMed: 737188]

7. Emken EA, Rohwedder WK, Dutton HJ, Dejarlais WJ, Adlof RO. Incorporation of deuterium-labeled *cis-* and *trans-*9-octadecenoic acids in humans: plasma, erythrocyte, and platelet phospholipids. Lipids 1979;14:547–554. [PubMed: 459721]

8. Emken EA, Dutton HJ, Rohwedder WK, Rakoff H, Adlof RO. Distribution of deuterium-labeled *cis-* and *trans-*12-octadecenoic acids in human plasma and lipoprotein lipids. Lipids 1980;15:864–871. [PubMed: 7442476]

9. Blomstrand R, Diczfalusy U, Sisfontes L, Svensson L. Influence of dietary partially hydrogenated vegetable and marine oils on membrane composition and function of liver microsomes and platelets in the rat. Lipids 1985;20:283–295. [PubMed: 4010485]

10. Hoy CE, Holmer G. Incorporation of *cis-* and *trans-*octadecenoic acids into the membranes of rat liver mitochondria. Lipids 1979;14:727–733. [PubMed: 530008]

11. Mensink RP, Katan MB. Effect of dietary trans fatty acids on high and low-density lipoprotein cholesterol levels in healthy subjects. N. Engl. J. Med 1990;323:439–445. [PubMed: 2374566]

12. Nestel P, Noakes M, Belling B, McArthur R, Clifton P, Janus E, Abbey M. Plasma lipoprotein lipid and Lp-[a] changes with substitution of elaidic acid for oleic acid in the diet. J. Lipid Res 1992;33:1029–1036. [PubMed: 1431582]

13. Zock PL, Katan MB. Hydrogenation alternatives: effects of trans fatty acids and stearic acid versus linoleic acid on serum lipids and lipoproteins in humans. J. Lipid Res 1992;33:399–410. [PubMed: 1569387]

14. Judd JT, Clevidence BA, Muesing RA, Wittes J, Sunkin ME, Podczasy JJ. Dietary trans fatty acids: effects on plasma lipids and lipoproteins of healthy men and women. Am. J. Clin. Nutr 1994;59:861–868. [PubMed: 8147331]

15. Katan MB, Zock PL, Mensink RP. Trans fatty acids and their effects on lipoproteins in humans. Annu. Rev. Nutr 1995;15:473–493. [PubMed: 8527230]

16. Willett WC, Stampfer MJ, Manson JE, Colditz GA, Speizer FE, Rosner BA, Sampson LA, Hennekens CH. Intake of trans fatty acids and risk of coronary heart disease among women. Lancet 1993;341:581–585. [PubMed: 8094827]

17. Kromhout D, Menotti A, Bloemberg B, Aravanis C, Blackburn H, Buzina R, Dontas AS, Fidanza F, Giampaoli S, Jansen A. Dietary saturated and trans fatty acids and cholesterol and 25-year mortality from coronary heart disease: the Seven Countries Study. PreV. Med 1995;24:308–315. [PubMed: 7644455]

18. Hu FB, Stampfer MJ, Rimm E, Ascherio A, Rosner BA, Spiegelman D, Willett WC. Dietary fat and coronary heart disease: a comparison of approaches for adjusting for total energy intake and modeling repeated dietary measurements. Am. J. Epidemiol 1999;149:531–540. [PubMed: 10084242]

19. Grundy SM, Ahrens EH Jr. The effects of unsaturated dietary fats on absorption, excretion, synthesis, and distribution of cholesterol in man. J. Clin. InVest 1970;49:1135–1152. [PubMed: 5422017]

20. Bjorntorp P. Rates of oxidation of different fatty acids by isolated rat liver mitochondria. J. Biol. Chem 1968;243:2130–2133. [PubMed: 5648428]

21. Clarke SD. Polyunsaturated fatty acid regulation of gene transcription: a molecular mechanism to improve the metabolic syndrome. J. Nutr 2001;131:1129–1132. [PubMed: 11285313]

22. Leventis R, Silvius JR. Use of cyclodextrins to monitor transbilayer movement and differential lipid affinities of cholesterol. Biophys. J 2001;81:2257–2267. [PubMed: 11566796]

23. Niu SL, Litman BJ. Determination of membrane cholesterol partition coefficient using a lipid vesicle-cyclodextrin binary system: effect of phospholipid acyl chain unsaturation and headgroup composition. Biophys. J 2002;83:3408–3415. [PubMed: 12496107]

24. Radhakrishnan A, McConnell HM. Chemical activity of cholesterol in membranes. Biochemistry 2000;39:8119–8124. [PubMed: 10889017]

25. Van Dijck PW, De Kruijff B, Van Deenen LL, De Gier J, Demel RA. The preference of cholesterol for phosphatidylcholine in mixed phosphatidylcholine-phosphatidylethanolamine bilayers. Biochim. Biophys. Acta 1976;455:576–587. [PubMed: 999929]

26. Demel RA, Jansen JW, Van Dijck PW, Van Deenen LL. The preferential interaction of cholesterol with different classes of phospholipids. Biochim. Biophys. Acta 1977;465:1–10. [PubMed: 836830]

27. Fugler L, Clejan S, Bittman R. Movement of cholesterol between vesicles prepared with different phospholipids or sizes. J. Biol. Chem 1985;260:4098–4102. [PubMed: 3980469]

28. Stillwell W, Ehringer WD, Dumaual AC, Wassall SR. Cholesterol condensation of α-linolenic and ç-linolenic acid-containing phosphatidylcholine monolayers and bilayers. Biochim. Biophys. Acta 1994;1214:131–136. [PubMed: 7918592]

29. Mitchell DC, Litman BJ. Effect of cholesterol on molecular order and dynamics in highly polyunsaturated phospholipid bilayers. Biophys. J 1998;75:896–908. [PubMed: 9675190]

30. Mitchell DC, Straume M, Miller JL, Litman BJ. Modulation of metarhodopsin formation by cholesterol-induced ordering of bilayer lipids. Biochemistry 1990;29:9143–9149. [PubMed: 2271584]

31. Niu SL, Mitchell DC, Litman BJ. Manipulation of cholesterol levels in rod disk membranes by methyl-β-cyclodextrin: effects on receptor activation. J. Biol. Chem 2002;277:20139–20145. [PubMed: 11889130]

32. Sakmar TP. Structure of rhodopsin and the superfamily of seven-helical receptors: the same and not the same. Curr. Opin. Cell Biol 2002;14:189–195. [PubMed: 11891118]

33. Litman BJ. Purification of rhodopsin by concanavalin A affinity chromatography. Methods Enzymol 1982;81:150–153. [PubMed: 7098858]

34. Miller JL, Fox DA, Litman BJ. Amplification of phosphodiesterase activation is greatly reduced by rhodopsin phosphorylation. Biochemistry 1986;25:4983–4988. [PubMed: 3021208]

35. Jackson ML, Litman BJ. Rhodopsin-egg phosphatidylcholine reconstitution by an octyl glucoside dilution procedure. Biochim. Biophys. Acta 1985;812:369–376. [PubMed: 3881128]

36. Barlett GR. Phosphorus Assay in Column Chromatography. J. Biol. Chem 1959;234:466–468. [PubMed: 13641241]

37. Shichi H. Spectrum and purity of bovine rhodopsin. Biochemistry 1970;9:1973–1977. [PubMed: 5442166]

38. Straume M, Litman BJ. Equilibrium and dynamic structure of large, unilamellar, unsaturated acyl chain phosphatidylcholine vesicles. Higher order analysis of 1,6-diphenyl-1,3,5-hexatriene and 1-[4-(trimethylammonio)phenyl]-6-phenyl-1,3,5-hexatriene anisotropy decay. Biochemistry 1987;26:5113–5120. [PubMed: 3663647]

39. Mitchell DC, Litman BJ. Molecular order and dynamics in bilayers consisting of highly polyunsaturated phospholipids. Biophys. J 1998;74:879–891. [PubMed: 9533699]

40. Straume M, Mitchell DC, Miller JL, Litman BJ. Interconversion of metarhodopsins I and II: a branched photointermediate decay model. Biochemistry 1990;29:9135–9142. [PubMed: 2271583]

41. Roach C, Feller SE, Ward JA, Shaikh SR, Zerouga M, Stillwell W. Comparison of Cis and Trans Fatty Acid Containing Phosphatidylcholines on Membrane Properties. Biochemistry 2004;43:6344–6351. [PubMed: 15147219]

42. Thomas PG, Verkleij AJ. The dissimilar interactions of the calcium antagonist flunarizine with different phospholipid classes and molecular species: a differential scanning calorimetry study. Biochim. Biophys. Acta 1990;1030:211–222. [PubMed: 2261484]

43. Albert AD, Yeagle PL. Phospholipid domains in bovine retinal rod outer segment disk membranes. Proc. Natl. Acad. Sci. U.S.A 1983;80:7188–7191. [PubMed: 6580636]

44. Bienvenue A, Bloom M, Davis JH, Devaux PF. Evidence for protein-associated lipids from deuterium nuclear magnetic resonance studies of rhodopsin-dimyristoylphosphatidylcholine recombinants. J. Biol. Chem 1982;257:3032–3038. [PubMed: 7061462]

45. Brown MF, Miljanich GP, Dratz EA. Proton spin-lattice relaxation of retinal rod outer segment membranes and liposomes of extracted phospholipids. Proc. Natl. Acad. Sci. U.S.A 1977;74:1978–1982. [PubMed: 266718]

46. Watts A, Volotovski ID, Marsh D. Rhodopsinlipid associations in bovine rod outer segment membranes. Identification of immobilized lipid by spin-labels. Biochemistry 1979;18:5006–5013. [PubMed: 228706]

47. Davis PJ, Keough KMW. Differential Scanning Calorimetric Studies of Aqueous Dispersions of Mixtures of Cholesterol with Some Mixed-Acid and Single-acid Phosphatidylcholines. Biochemistry 1983;22:6334–6340.

48. Polozova A, Litman BJ. Cholesterol dependent recruitment of di22:6-PC by a G protein-coupled receptor into lateral domains. Biophys. J 2000;79:2632–2643. [PubMed: 11053136]

49. Lamola AA, Yamane T, Zipp A. Effects of detergents and high pressure upon the metarhodopsin I-metarhodopsin II equilibrium. Biochemistry 1974;13:738–745. [PubMed: 4855767]

50. Litman BJ, Mitchell DC. A role for phospholipid polyunsaturation in modulating membrane protein function. Lipids 1996;31:S193–S197. [PubMed: 8729118]

51. Brown MS, Goldstein JL. A receptor-mediated pathway for cholesterol homeostasis. Science 1986;232:34–47. [PubMed: 3513311]

52. Brown MS, Goldstein JL. A proteolytic pathway that controls the cholesterol content of membranes, cells, and blood. Proc. Natl. Acad. Sci. U.S.A 1999;96:11041–11048. [PubMed: 10500120]

53. Brown AJ, Sun L, Feramisco JD, Brown MS, Goldstein JL. Cholesterol addition to ER membranes alters conformation of SCAP, the SREBP escort protein that regulates cholesterol metabolism. Mol. Cell 2002;10:237–245. [PubMed: 12191470]

54. Yang T, Espenshade PJ, Wright ME, Yabe D, Gong Y, Aebersold R, Goldstein JL, Brown MS. Crucial step in cholesterol homeostasis: sterols promote binding of SCAP to INSIG-1, a membrane protein that facilitates retention of SREBPs in ER. Cell 2002;110:489–500. [PubMed: 12202038]
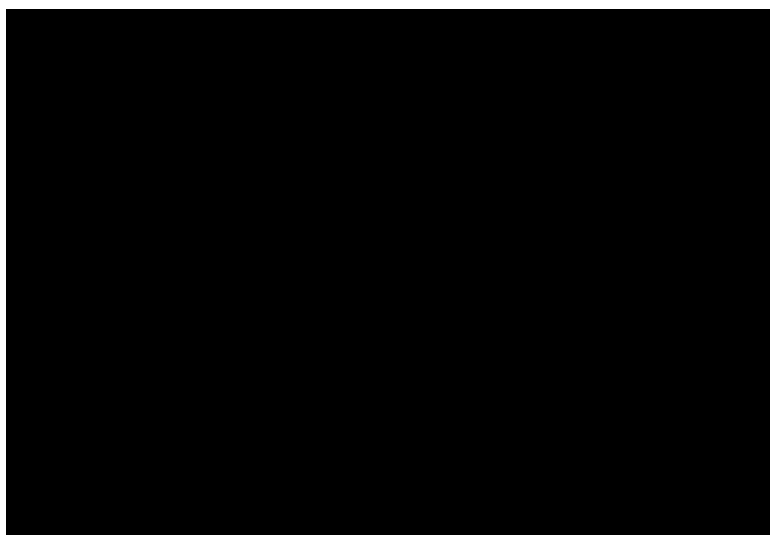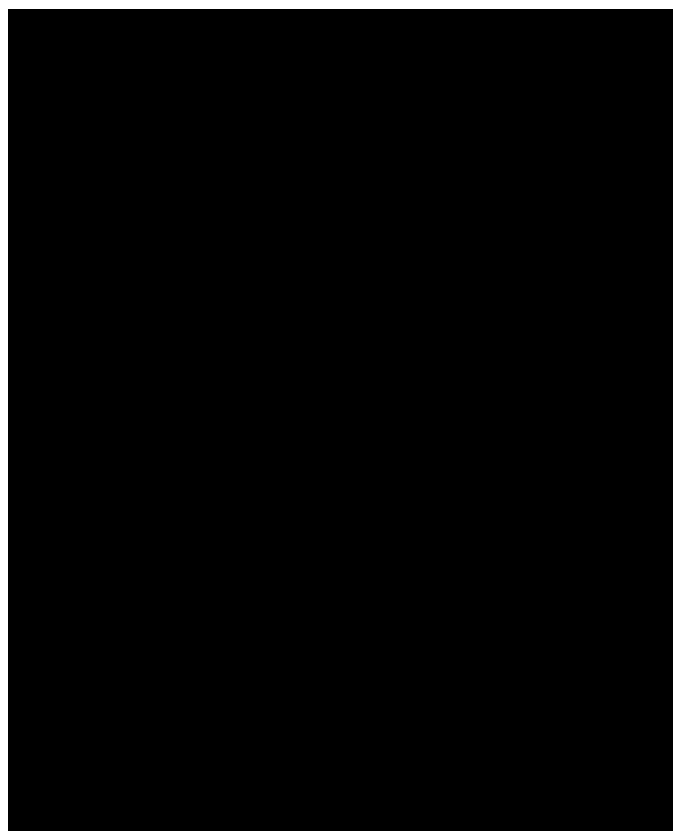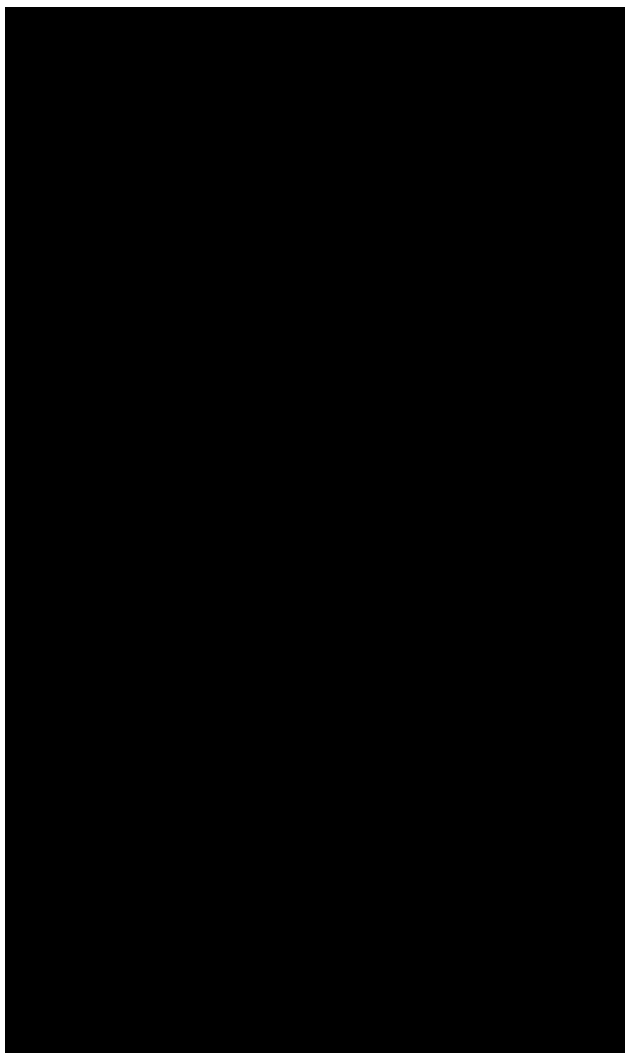
FIGURE 1:
Chemical structures of trans and cis fatty acids. Modeling of elaidic acid or 9-*trans*-octadecenoic acid (top) and oleic acid or 9-*cis*-octadecenoic (bottom). The trans isomer adopts a linear configuration, while the cis isomer is in a bent configuration.

FIGURE 2:
Lipid dependence of membrane cholesterol partitioning. Equilibrium cholesterol partition coefficient was determined between LUV that contains either cis (open bars) or trans (hatched bars) fatty acid-derived phospholipids and methyl-β-cyclodextrin (CD) (A). Cholesterol partition coefficient (K_{cis}^{trans}) between trans and its corresponding *cis*-phospholipid (B) was derived from measurements similar to those shown in panel A.

FIGURE 3:
DSC scans of reconstituted rhodopsin-containing vesicles. Shown in panel A are thermal transitions of rhodopsin in di-18:1n9(c) PC vesicles (···) and in di-18:1n9(t) PC vesicles (---). The thermal transitions were analyzed according to a two-state transition model, shown as (—) for both lipid vesicles. Shown in panel B are phospholipid phase transitions in rhodopsin-containing di-18:1n9(c)PC vesicles (···) and rhodopsin-containing di-18:1n9-(t)PC vesicles before (---) and after (—) rhodopsin is thermally denatured. Also shown in panel B is the di-18:1n9(t)PC phase transition in pure di-18:1n9(t)PC vesicles without rhodopsin (-···-). It was scaled down by a factor of 2 for clarity.

FIGURE 4:
Metarhodopsin I (MI) and metarhodopsin II (MII) equilibrium difference spectra in reconstituted vesicles. Spectra were acquired in rhodopsin-containing vesicles consisting of di-18:1n9-(c)PC (O) and di-18:1n9(t)PC (·) in pH 7.0 PBS buffer at 37°C. The dashed and solid lines were the corresponding deconvoluted spectra of MI (480 nm) and MII (385 nm) in di-18:1n9(c)PC and di-18:1n9(t)PC, respectively. The equilibrium constants for MI-MII were derived from these spectra.

FIGURE 5:
Trans fatty acid-derived phospholipids reduced rhodopsin activation. MI-MII equilibrium constants (K_{eq}) were derived from equilibrium spectra as shown in Figure 4. Shown here are K_{eq} values from reconstituted rhodopsin-containing vesicles consisting of di-18:1n9(c)PC (open bar) and di-18:1n9(t)PC (hatched bar). The top panel was measured at 37°C, where both di-18:1n9(c)PC and di-18:1n9(t)PC are in the liquid crystalline phase, while the bottom panel was acquired at 5°C, where di-18:1n9(c)PC is in the liquid crystalline phase and di-18:1n9(t) PC is in the gel phase.
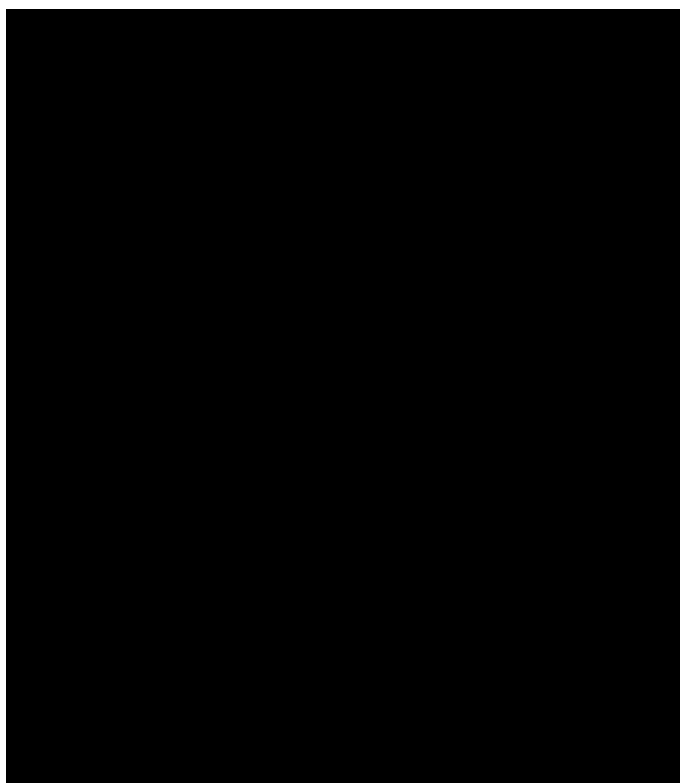
FIGURE 6:
van't Hoff plot of the MI-MII equilibrium constants. Plot of ln K_{eq} from reconstituted rhodopsin vesicles consisting of di-18:1n9(c)PC (O) and di-18:1n9(t)PC (▲)vs1/T. The dashed and solid lines were the corresponding linear fits of the data. The open triangle data point was excluded in the linear fit since di-18:1n9-(t)PC was below its phase transition at 5°C.

Table 1:

Time-Resolved DPH Fluorescence Measurements in Lipid Vesicles Consisting of di-18:1n9(c)PC and di-18:1n9 (t)PC[a]

	di-18:1n9(c)PC	di-18:1n9(t)PC
$\langle\tau\rangle$, ns	7.37 ± 0.02	8.28 ± 0.23
$\langle\phi\rangle$, ns	1.49 ± 0.03	1.91 ± 0.07
$D_\perp$, ns^{-1}	0.15 ± 0.00	0.14 ± 0.00
f_v	0.18 ± 0.01	0.12 ± 0.00

[a] Time-resolved fluorescence decay and polarization data were acquired at 37 °C. The standard deviations were derived from three independent measurements.

Table 2:

DSC Summary of the Gel-to-Liquid Crystalline Phase Transition of Lipid and Thermal Denaturation of Rhodopsin in Lipid Vesicles

	T_m (°C)[a]	ΔH (kcal/mol)[a]
Protein transition		
di-18:1n9(c)PC	68.0 ± 0.02	160.6 ± 1.1
di-18:1n9(t)PC	69.7 ± 0.01	198.5 ± 1.2
Lipid transition		
di-18:1n9(t)PC		
first heating scan	9.9 ± 0.02	nd[b]
	10.6 ± 0.01	nd[b]
second heating scan	11.2 ± 0.00	6.37 ± 0.03
di-18:19(t)PC (lipid only)	11.5 ± 0.00	8.30 ± 0.13

[a]Numbers were expressed ± SD.

[b]Not determined.

Table 3:

Thermodynamic Parameters for the MI-MII Equilibrium

	ΔH_{vh} (kcal/mol)	ΔS (cal/mol K)	r^2
cis	10.44 ± 0.42	33.44 ± 1.45	0.997
trans (>T_m)	12.45 ± 0.18	39.42 ± 0.62	1.000